Graphene nanoribbon based spaser

Oleg L. Berman,[1,2] Roman Ya. Kezerashvili,[1,2] and Yurii E. Lozovik[3,4]

[1]*Physics Department, New York City College of Technology, The City University of New York, Brooklyn, New York 11201, USA*

[2]*The Graduate School and University Center, The City University of New York, New York, New York 10016, USA*

[3]*Institute of Spectroscopy, Russian Academy of Sciences, 142190 Troitsk, Moscow Region, Russia*

[4]*Moscow Institute of Physics and Technology (State University), 141700, Dolgoprudny, Russia*

(Received 22 September 2013; revised manuscript received 17 November 2013; published 19 December 2013)

A novel type of spaser with the net amplification of surface plasmons (SPs) in a doped graphene nanoribbon is proposed. The plasmons in the THz region can be generated in a doped graphene nanoribbon due to nonradiative excitation by emitters like two level quantum dots located along a graphene nanoribbon. The minimal population inversion per unit area, needed for the net amplification of SPs in a doped graphene nanoribbon, is obtained. The dependence of the minimal population inversion on the surface plasmon wave vector, graphene nanoribbon width, doping, and damping parameters necessary for the amplification of surface plasmons in the armchair graphene nanoribbon is studied.

DOI: 10.1103/PhysRevB.88.235424 PACS number(s): 78.67.Wj, 42.50.Nn, 73.20.Mf, 73.21.−b

I. INTRODUCTION

The essential achievements in nanoscience and nanotechnology during the past decade lead to great interest in studying nanoscale optical fields. The phenomenon of surface plasmon amplification by stimulated emission of radiation (spaser) was proposed in Ref. 1 (see also Refs. 2 and 3). Spaser generates coherent high-intensity fields of selected surface plasmon (SP) modes that can be strongly localized on the nanoscale. The properties of localized plasmons are reviewed in Refs. 4–7. The spaser consists of an active medium formed by two-level systems [semiconductor quantum dots (QDs) or organic molecules] and a plasmon resonant nanosystem where the surface plasmons are excited. The emitters transfer their excitation energy by radiationless transitions through near fields to a resonant plasmon nanosystem.

By today theoretical and experimental studies are focused on metal-based spasers, where surface plasmons are excited in different metallic nanostructures of different geometric shapes. A spaser consisting of the nanosystem formed by the V-shaped silver nanoinclusion embedded in a dielectric host containing the PbS and PbSe QDs was considered in Ref. 1. A spaser formed by a silver spherical nanoshell on a dielectric core with a radius of 10–20 nm, and surrounded by two dense monolayers of nanocrystal QDs, was considered in Ref. 8. The SPs propagating along the bottom of the groove (channel) in the metal surface were studied in Ref. 9. The SPs are assumed to be coherently excited by a linear chain of QDs at the bottom of the channel. It was shown that for the realistic values of the system parameters, the gain can exceed the loss and plasmonic lasing in a ring or linear channels in the silver surface surrounded by a linear chain of CdSe QDs can occur. In Refs. 10–13 the spaser formed by the metal sphere surrounded by the two-level quantum dot was studied theoretically. The spaser consisting of the spherical gain core, containing two-level systems, coated with a metal spherical plasmonic shell, was theoretically analyzed in Ref. 14. The experimental study of the spaser formed by 44-nm-diameter nanoparticles with the gold spherical core surrounded by a dye-doped silica shell was performed in Refs. 15 and 16. In this experiment the emitters were formed by the dye-doped silica shell instead of QDs. It was demonstrated that a two-dimensional array of a certain class of plasmonic resonators supporting coherent current excitations with a high quality factor can act as a planar source of spatially and temporally coherent radiation.[17] This structure consists of a gain medium slab supporting a regular array of silver asymmetric split-ring resonators. The spaser formed by 55-nm-thick gold film with the nanoslits located on the silica substrate surrounded by PbS QDs was experimentally studied in Ref. 18. Room temperature spasing of surface plasmon polaritons at 1.46 μm wavelength has been demonstrated by sandwiching a gold-film plasmonic waveguide between optically pumped InGaAs quantum-well gain media.[19]

Since plasmons can also be excited in graphene, and damping in graphene is much less than in metals,[20–22] we propose to use a graphene nanoribbon surrounded by semiconductor QDs as the nanosystem for the spaser. Plasmons in graphene provide a suitable alternative to plasmons in noble metals, because they exhibit much tighter confinement and relatively long propagation distances, with the advantage of being highly tunable via electrostatic gating.[23] Besides, the graphene-based spaser can work in the THz frequency regime. Recently there were many experimental and theoretical studies devoted to graphene known by unusual properties in its band structure.[24,25] The properties of plasmons in graphene were discussed in Refs. 26–29. The electronic properties of graphene nanoribbons depend strongly on their size and geometry.[30,31] The frequency spectrum of oblique terahertz plasmons in graphene nanoribbon arrays was obtained.[32] Besides, a graphene-based spaser seems to meet the new technological needs, since it works at the infrared (IR) frequencies, while the metal-based spaser works at the higher frequencies. Let us mention that the graphene-based photonic two- and one-dimensional crystals proposed in Refs. 33 and 34 also can be used effectively as the frequency filters and waveguides for the far infrared region of the electromagnetic spectrum.

In this paper we propose the graphene nanoribbon based spaser consisting of a graphene nanoribbon surrounded by semiconductor QDs. The QDs excited by the laser pumping nonradiatively transfer their excitation to the SPs localized at the graphene nanoribbon, which results in an increase of intensity of the SP field. Our preliminary results were reported

at the 2013 APS March Meeting.[35] Below we calculate the minimal population inversion that is the difference between the surface densities of QDs in the excited and ground states needed for the net SP amplification and study its dependence on the surface plasmon wave vector, graphene nanoribbon width at fixed temperature for different doping, and damping parameters for the armchair graphene nanoribbon.

The paper is organized in the following way. In Sec. II the minimal population inversion for the graphene-based spaser is obtained. The discussion of the results and conclusions follow in Sec. III.

II. SURFACE PLASMON AMPLIFICATION

The system under consideration is the graphene nanoribbon, which is the stripe of graphene at $z = 0$ in the plane (x, y), that is infinite in the x direction and has the width W in the y direction. This nanoribbon is surrounded by the deposited dense monolayer of nanocrystal quantum dots with the dielectric constant ε_d at $z < 0$ and $z > 0$. When the quantum dots are optically pumped, the resonant nonradiative transmission occurs by creating a surface plasmon localized in the graphene nanoribbon. Our goal is to show that amplification by QDs can exceed absorption of the surface plasmon in the graphene nanoribbon. As a result we obtain an increase of intensity of the surface plasmon field. In other words, the competition between the gain and the loss of the surface plasmon field in the graphene nanoribbon will result in favor of the gain.

Below we derive the expression for the minimal population inversion per unit area N_c, needed for the net amplification of SPs in a doped graphene nanoribbon. We obtain this expression from the condition that for the regime of the plasmon amplification the rate $\partial\bar{U}/\partial t$ of the transfer of the average energy of the QDs is greater than the heat released per unit time $\partial Q/\partial t$ due to the absorption of the energy of the plasmon field in the graphene nanoribbon.

Let us start from the Poynting theorem for the rate of the transferred energy density from a region of space $\partial\mathcal{W}/\partial t = -\mathrm{div}\vec{S}$, where $\vec{S}$ is the Poynting vector and assume that the plasmon frequency equals the QD transition frequency. From the other side, the rate of the transferred energy related to the rates of the average energy of the QDs and the heat released due to the absorption of the energy by the graphene nanoribbon can be presented as

$$-\frac{\partial}{\partial t}\int \mathcal{W}dV = \frac{\partial\bar{U}}{\partial t} - \frac{\partial Q}{\partial t}, \tag{1}$$

where V is the volume of the system. Therefore, from the Poynting theorem we have the following expression:

$$\int \mathrm{div}\vec{S}dV = \frac{\partial\bar{U}}{\partial t} - \frac{\partial Q}{\partial t}. \tag{2}$$

When the plasmon frequency ω equals the QD transition frequency, we assume $\vec{E} \sim \exp(-i\omega t)$, $\vec{H} \sim \exp(-i\omega t)$, and $\vec{P} \sim \exp(-i\omega t)$, where $\vec{E}$ and $\vec{H}$ are the electric and demagnetizing fields, correspondingly, of the graphene nanoribbon plasmon, and $\vec{P}$ is the polarization of QDs, which is the average total dipole moment of the unit of the volume V. Then it can be easily shown that the Poynting vector is given by[36]

$$\vec{S} = \tfrac{1}{2}\mathrm{Re}[\vec{E} \times \vec{H}^*]. \tag{3}$$

Using Maxwell equations and the electric displacement field $\vec{D} = \vec{P} + \varepsilon\vec{E}$, where ε is the dielectric function of graphene nanoribbon, the following expression for $\int \mathrm{div}\vec{S}dV$ can be derived:

$$\int \mathrm{div}\vec{S}dV = \frac{\omega}{2}\int \mathrm{Im}(\vec{E}\cdot\vec{P}^*)dV - \frac{\omega}{2}\int \mathrm{Im}\varepsilon|\vec{E}|^2dV. \tag{4}$$

In Eq. (4) the first term on the right-hand side corresponds to the rate of the polarization energy of the quantum dots, while the second term corresponds to the rate of the heat released from the graphene nanoribbon.

Let us consider now each term on the left-hand side of Eq. (4) separately. The excitation causing the generation of plasmons in the graphene nanoribbon comes from the transitions in the QDs between the excited and ground states. Therefore, the rate of the transfer of the average energy $\bar{U}$ of the QDs characterized by the dipole moment is given by

$$\frac{\partial\bar{U}}{\partial t} = \frac{\omega}{2}\int \mathrm{Im}(\vec{E}\cdot\vec{P}^*)dV, \tag{5}$$

where the relation between the polarization of QDs $\vec{P}$ and electric field of the graphene nanoribbon plasmon $\vec{E}$ has the form[9]

$$\vec{P} = -ik\frac{\tau_p|\mu|^2 n}{\hbar}\vec{E}, \tag{6}$$

where $k = 9 \times 10^9\ \mathrm{N\,m^2/C^2}$, n is the difference between the concentrations of the quantum dots in the excited and ground states per unit of volume, τ_p is the inverse linewidth, and μ is the average off-diagonal element of the dipole moment of a single QD.

Substituting Eq. (6) into Eq. (5), we obtain the rate of the transfer of the average energy of the QDs,

$$\frac{\partial\bar{U}}{\partial t} = \omega k\frac{\tau_p|\mu|^2}{2\hbar}\int n|\vec{E}|^2dV. \tag{7}$$

We assume that the distances between the quantum dots are small, so their effect on a plasmon is the same as that of a continuous (constant) gain distribution along the graphene nanoribbon. We consider the two-dimensional graphene nanoribbon at $z = 0$ and assume it is infinite in the x direction, has the width W in the y direction, and is surrounded by the monolayer of uniformly distributed quantum dots. Therefore, for n we have $n = N_0\eta(y, -W/2, W/2)\delta(z)$, where N_0 is the difference between the numbers of the excited and ground state quantum dots per unit area, and $\eta(y, -W/2, W/2) = 1$ at $-W/2 \leqslant y \leqslant W/2$, and $\eta(y, -W/2, W/2) = 0$ at $y < -W/2$ and $y > W/2$. Thus, we obtain from Eq. (7)

$$\begin{aligned}\frac{\partial\bar{U}}{\partial t} &= \omega k\frac{\tau_p|\mu|^2}{2\hbar}\int_{-\infty}^{+\infty}dx\int_{-\infty}^{+\infty}dy \\ &\quad\times\int_{-\infty}^{+\infty}dz N_0\eta(y, -W/2, W/2)\delta(z)|\vec{E}(x,y,z)|^2 \\ &= \omega k\frac{\tau_p|\mu|^2 N_0}{2\hbar}\int_{-W/2}^{+W/2}dy\int_{-\infty}^{+\infty}dx|\vec{E}(x,y,0)|^2.\end{aligned} \tag{8}$$

Taking into account the spatial dispersion of the dielectric function in the graphene nanoribbon,[30,31] we use the following

expression for the rate of the heat $\partial Q/\partial t$ released due to the absorption of the energy of the plasmon field in the graphene nanoribbon[4,37]:

$$\frac{\partial Q}{\partial t} = \frac{\omega}{2}\int \mathrm{Im}\varepsilon(\omega,q_x)\eta(y,-W/2,W/2)|\vec{E}|^2 dV = \frac{\omega}{2}\mathrm{Im}\varepsilon(\omega,q_x)\int_{-\infty}^{+\infty}dx\int_{-W/2}^{+W/2}dy\int_{-\infty}^{+\infty}dz|\vec{E}(x,y,z)|^2, \tag{9}$$

where $\mathrm{Im}\varepsilon(\omega,q_x)$ is the imaginary part of the dielectric function $\varepsilon \equiv \varepsilon(\omega,q_x)$ of graphene nanoribbon given by Eq. (A1).

The plasmons in a graphene nanoribbon are excited due to the radiation caused by the transitions from the excited state to the ground state on the QDs. Therefore, according to the conservation of energy, the regime of the amplification of the plasmons in the graphene nanoribbon is established, if the rate of the transfer of the average energy $\partial\bar{U}/\partial t$ of the QDs given by Eq. (8) is greater than the heat released rate $\partial Q/\partial t$ due to the absorption of the energy of the plasmon field in the graphene nanoribbon:

$$\frac{\partial\bar{U}}{\partial t} > \frac{\partial Q}{\partial t}. \tag{10}$$

Substituting Eqs. (8) and (9) into Eq. (10) we get

$$k\frac{\tau_p|\mu|^2N_0}{\hbar}\int_{-W/2}^{+W/2}dy\int_{-\infty}^{+\infty}dx|\vec{E}(x,y,0)|^2 > \mathrm{Im}\varepsilon(\omega,q_x)\int_{-\infty}^{+\infty}dx\int_{-W/2}^{+W/2}dy\int_{-\infty}^{+\infty}dz|\vec{E}(x,y,z)|^2. \tag{11}$$

From Eq. (11) one can obtain the condition for the difference between the surface densities of the quantum dots in the excited and ground state corresponding to the amplification of plasmons:

$$N_0 > N_c = \frac{\mathrm{Im}\varepsilon(\omega,q_x)\int_{-\infty}^{+\infty}dx\int_{-W/2}^{+W/2}dy\int_{-\infty}^{+\infty}dz|\vec{E}(x,y,z)|^2}{k\frac{\tau_p|\mu|^2}{\hbar}\int_{-\infty}^{+\infty}dx\int_{-W/2}^{+W/2}dy|\vec{E}(x,y,0)|^2}, \tag{12}$$

where N_c is the critical density of the QDs required for the amplification of the plasmons. The evaluation of the integrals in Eq. (12) requires the knowledge of the electric field of a plasmon in a graphene nanoribbon. The electric field of a plasmon in a graphene nanoribbon is derived in Appendix B. Using Eq. (B9) for the electric field of a plasmon, we have

$$|\vec{E}(x,y,0)|^2 = E_0^2\left[2q_x^2\cos^2(q_y y)+q_y^2\right], \tag{13}$$

$$|\vec{E}(x,y,z)|^2 = E_0^2e^{-2\alpha|z|}\left[2q_x^2\cos^2(q_y y)+q_y^2\right], \tag{14}$$

where $\alpha = \sqrt{q_x^2+q_y^2}$ and for the armchair nanoribbon we have $q_{ym} = 2\pi/(3a_0)\,[(2M+1+m)/(2M+1)]$ at the width $W = (3M+1)a_0$,[30] where a_0 is the graphene lattice constant, and m is the integer. We use $m = 1$. Substituting Eqs. (13) and (14) into Eq. (12), we obtain

$$N_0 > N_c = \frac{2\hbar\mathrm{Im}\varepsilon(\omega,q_x)\int_{-\infty}^{+\infty}dx\int_{-W/2}^{+W/2}dy\int_0^{+\infty}dze^{-2\alpha z}\left[2q_x^2\cos^2(q_y y)+q_y^2\right]}{k\tau_p|\mu|^2\int_{-\infty}^{+\infty}dx\int_{-W/2}^{+W/2}dy\left[2q_x^2\cos^2(q_y y)+q_y^2\right]}. \tag{15}$$

Finally from Eq. (15) we obtain

$$N_0 > N_c = \frac{\hbar\mathrm{Im}\varepsilon(\omega,q_x)}{\alpha k\tau_p|\mu|^2}. \tag{16}$$

Using Eqs. (A1) and (A2) one can find $\mathrm{Im}\varepsilon(q_x,\omega)$:

$$\mathrm{Im}\varepsilon(q_x,\omega) = -\frac{V_{0,0}(q_x)f_1(q_x,\beta,\mu_g)g_s v_F q_x\omega\gamma}{\pi\hbar\left[\left(\omega^2-v_F^2q_x^2\right)^2+\omega^2\gamma^2\right]}, \tag{17}$$

where v_F is the Fermi velocity of electrons in graphene, and γ is the damping rate for the graphene nanoribbon. The plasmon frequency ω can be obtained at $\gamma = 0$ from the condition $\mathrm{Re}\varepsilon(q_x,\omega) = 0$ using Eqs. (A1) and (A2):

$$\omega^2 = v_F^2q_x^2 - \frac{V_{0,0}(q_x)f_1(q_x,\beta,\mu_g)g_s v_F q_x}{\pi\hbar}. \tag{18}$$

To perform the calculations, one should calculate the critical density N_c using Eq. (16). N_c is a function of the wave vector q_x, the graphene nanoribbon width W, temperature T, and electron concentration n_0 determined by the doping.

The analysis of Eq. (17) shows that $\mathrm{Im}\varepsilon(q_x,\omega)$ depends on the damping rate γ. It is likely the damping rate γ will be affected by the scattering of charge carriers in doped graphene on the nearby quantum dots, thus making γ dependent on N_0. Therefore, the solution of the inequality (11) for N_0 would be highly nontrivial and the inequality (16) is obtained by assuming that the electron mean free path is much larger than the average distance between the quantum dots, and thus the parameter γ represents the average damping rate. In the calculations below we use $\gamma = \tau^{-1}$, where τ is a dissipation time from Refs. 38–41.

III. RESULTS AND DISCUSSION

For our calculations we use the following parameters for the PbS and PbSe QDs. Since the typical energy corresponding to the transition between the ground and excited electron states for the PbS and PbSe QDs synthesized with the radii from 1 to 8 nm can be 0.7 eV, we use $\tau_p \approx$ 5.9 fs, and $|\mu| = 1.9\times10^{-17}$ esu = 19 D (1 D = 10^{-18} esu,

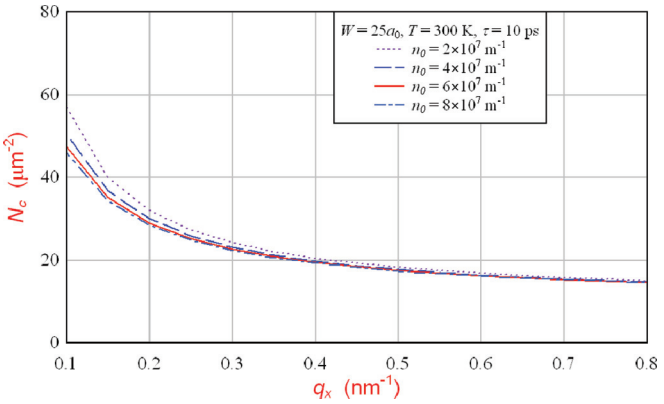

FIG. 1. (Color online) The dependence of the critical density of the QDs N_c on the wave vector q_x for the different 1D doping electron densities n_0 at the fixed width of the nanoribbon W, temperature T, and dissipation time τ corresponding to the damping.

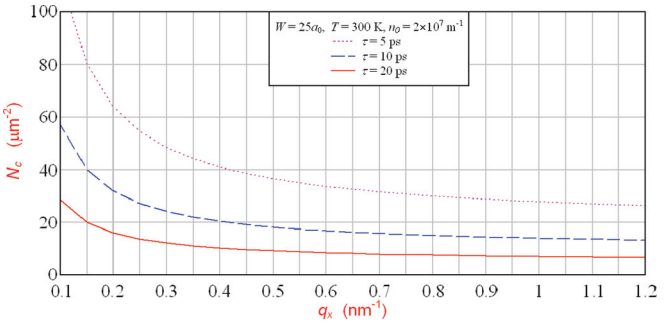

FIG. 2. (Color online) The dependence of the critical density of the QDs N_c on the wave vector q_x for the different dissipation time τ corresponding to the damping at the fixed width of the nanoribbon W, temperature T, and 1D doping electron density n_0.

$1\,\mathrm{D} = 3.33564 \times 10^{-30}\,\mathrm{C\,m}$).[42] Let us mention that the typical frequency corresponding to the transition between the ground and excited electron states for the PbS and PbSe QDs, which is $f \approx 170$ THz, matches the resonance with the plasmon frequency in the armchair graphene nanoribbon.[31] Therefore, the PbS and PbSe QDs can be used for the spaser considered here. The damping in graphene $\gamma = \tau^{-1}$ determined by the dissipation time τ is assumed to be either $\tau = 1$ ps or $\tau = 10$ ps or $\tau = 20$ ps.[38–41] The optical magnetoabsorption experiments for graphene in magnetic field demonstrate that the Landau level broadening allows us to estimate $\tau \approx 20$ ps.[38] The values of τ used in our calculations are close to the experimental quantities. Let us also mention that in the calculations below we use for the one-dimensional (1D) doping electron density n_0 the values of the same order of magnitude as in Ref. 31 (see Appendix A).

The dependence of the critical density of the QDs N_c required for the amplification of the signal on the wave vector q_x for the different 1D doping electron densities n_0 at the fixed width of the nanoribbon, temperature, and dissipation time τ corresponding to the damping, obtained using Eq. (16) is presented in Fig. 1. According to Fig. 1, N_c decreases as q_x and n_0 increase. Let us mention that at q_x larger than 0.4 nm^{-1} there is almost no difference between the values of N_c corresponding to the different 1D doping electron densities n_0, and for large q_x N_c converges to approximately 15 μm^{-2}. Since the critical density of the QDs N_c is a decreasing function of doping electron density n_0, which is nonuniform across the width of a graphene nanoribbon,[43,44] to be on the safe side we use in our calculations the minimal value of n_0 across the width. In this case the calculated value of N_c corresponds to the amplification regime across the entire graphene nanoribbon. In Fig. 2 the dependence of the critical density of the QDs N_c required for the amplification of the signal on the wave vector q_x for the different dissipation time corresponding to the damping at the fixed width of the nanoribbon, temperature, and 1D doping electron densities is shown. As it follows from Fig. 2, N_c decreases as q_x and τ increase. This means that higher damping corresponds to higher N_c. According to Fig. 2, starting with $q_x \approx 1.0$ nm^{-1}, N_c depends very weakly on q_x, converging to some constant values that depend on the value of τ. The dependence of the critical density of the QDs N_c required for the amplification of the signal on the width of the nanoribbon W at the different wave vector for the fixed dissipation time corresponding to the damping, temperature, and 1D doping electron densities obtained using Eq. (16) is displayed in Fig. 3. From Fig. 3 we can conclude that N_c increases as W increases and decreases as q_x increases. When W increases, the values of N_c strongly depend on q_x. The dependence of the critical density of the QDs N_c required for the amplification of the signal on the frequency f at the different dissipation time corresponding to the damping for the fixed temperature and 1D doping electron density is shown in Fig. 4. As it is demonstrated in Fig. 4, N_c increases as f and τ decrease. According to Fig. 4, starting with $f \approx 160$ THz, N_c depends very weakly on the frequency and converges to some constant values that depend on the value of τ. The dependence of the plasmon frequency f on the width of the nanoribbon W, for the different wave vectors at the fixed dissipation time corresponding to the damping, temperature, and 1D doping electron density obtained using Eq. (18), is presented in Fig. 5. According to Fig. 5, the plasmon frequency f increases as q_x increases and the width of the nanoribbon W decreases. If in Eq. (16) the imaginary part of the dielectric function would not depend on the width W, N_c would not depend on W. However, due to the complicated dependence of $\mathrm{Im}\varepsilon(\omega, q_x)$

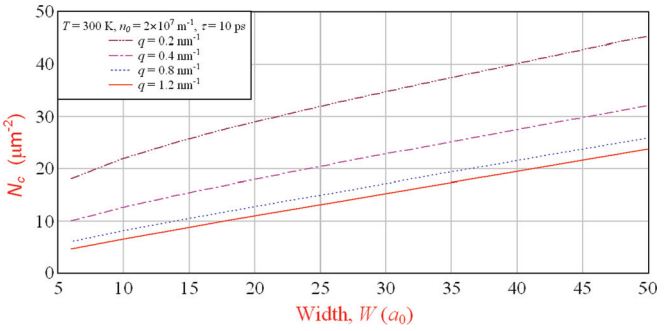

FIG. 3. (Color online) The dependence of the critical density of the QDs N_c on the width of the nanoribbon W at the different wave vector q_x for the fixed dissipation time τ corresponding to the damping, temperature T, and 1D doping electron densities n_0.

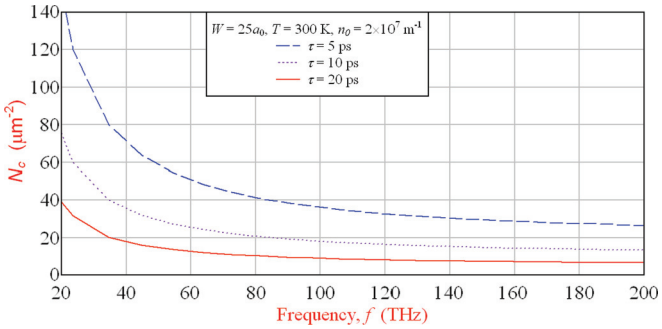

FIG. 4. (Color online) The dependence of the critical density of the QDs N_c on the frequency f at the different dissipation time τ corresponding to the damping for the fixed width W, temperature T, and 1D doping electron density n_0.

on W through $V_{0,0}(q_x)$ given by Eq. (A6), this dependence exists. For the damping time we use $\tau = 5$ ns, $\tau = 10$ ns, and $\tau = 20$ ns, because such damping for graphene was obtained in the experimental studies.[38–41] One can conclude from Figs. 2 and 4 that N_c decreases when the damping time τ increases.

Let us mention that we used the parameters for the PbS and PbSe QDs to calculate N_c, because among different materials for the QDs the PbS and PbSe QDs demonstrate the lowest transition frequency,[45] which can be in the resonance with the plasmon in graphene nanoribbon in the IR region of spectrum. According to Ref. 18, the transition frequency for the QDs depends on the radius of the QDs. The PbS QDs with the radii 2–5 nm have the transition frequencies 231 and 194 THz.[18] For our calculations we use the PbS and PbSe QDs synthesized with the radii up to 8 nm, which can provide the transition frequency $f \approx 170$ THz.[42] Let us mention that changing the radius of the QDs, we can change the frequency of the QDs resonant to the plasmon frequency in graphene nanoribbon controlled by the wave vector q_x, and, therefore, we can control N_c by the radius of the QDs. The density of the PbS QDs with the diameter 3.2 nm applied for the amplification of plasmons in a gold film in the experiment[18] was 4×10^6 μm^{-2}. According to Figs. 1–4, in the graphene nanoribbon-based spaser there are the possibilities to achieve much fewer densities of the PbS QDs necessary for amplification than in the gold film-based spaser.

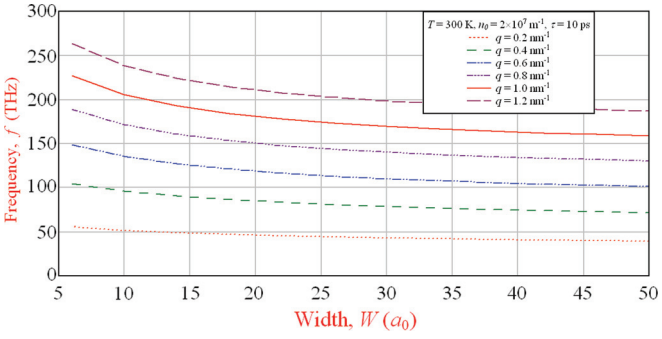

FIG. 5. (Color online) The dependence of the plasmon frequency f on the width of the nanoribbon W, for the different wave vectors q_x at the fixed dissipation time τ corresponding to the damping, temperature T, and 1D doping electron density n_0.

Let us mention that in our calculations we take into account the temporal and spatial dispersion of the dielectric function of graphene nanoribbon in the random phase approximation.[30,31] The effects of spatial dispersion are very important for the properties of a spaser based on a flat metal nanofilm.[46] Taking into account the spatial dispersion of the dielectric function of a metal surface in the local random phase approximation allows us to conclude that the strong interaction of the QD with unscreened metal electrons in the surface nanolayer causes enhanced relaxation due to the surface plasmon excitation and Landau damping in a spaser based on a flat metal nanofilm.[46] And we assume that taking into account the spatial dispersion of the dielectric function of the graphene nanoribbon is also very important to calculate the minimal population inversion needed for the net SP amplification in the graphene nanoribbon based spaser.

The advantages of the graphene nanoribbon based spaser are a wide frequency generation region from THz up to IR, the small damping, the low threshold for pumping, and possibility of control by the gate. While we perform our calculations for IR radiation corresponding to the transition frequencies 170 THz, the graphene-based spaser can work at the frequencies much below this one including the THz regime.

ACKNOWLEDGMENTS

The authors are grateful to M. I. Stockman for discussions. The work was supported by PSC CUNY under Grant No. 65572-00 43. Yu. E. L. was supported by Program of Basic Research of HSE.

APPENDIX A: THE DIELECTRIC FUNCTION OF THE ARMCHAIR GRAPHENE NANORIBBON

For the armchair graphene nanoribbon the dielectric function $\varepsilon(q_x,\omega) \equiv \varepsilon_{00}(q_x,\omega,\beta,\mu_g)$ in the one-band approximation within random phase approximation is given by[31]

$$\varepsilon_{00}(q_x,\omega,\beta,\mu_g) = 1 - V_{0,0}(q_x)\Pi_{0,0}(q_x,\omega,\beta,\mu_g), \quad \text{(A1)}$$

where $V_{0,0}(q_x)$ is the Coulomb matrix element, and the polarizability $\Pi_{0,0}(q_x,\omega)$ can be approximated by

$$\Pi_{0,0}(q_x,\omega,\beta,\mu_g) = -\frac{g_s}{\pi}\frac{\hbar v_F q_x}{\hbar^2[\omega(\omega+i\gamma)-(v_F q_x)^2]} f_1(q_x,\beta,\mu_g), \quad \text{(A2)}$$

with

$$f_1(q_x,\beta,\mu_g) = \frac{1}{\hbar\beta v_F}\left[-\beta\hbar v_F q_x + 2\ln\left(\frac{1+e^{-\beta\mu_g}}{1+e^{-\beta(\hbar v_F q_x+\mu_g)}}\right)\right], \quad \text{(A3)}$$

where $g_s = 2$ is the spin degeneracy factor, $\beta = 1/(k_B T)$, k_B is the Boltzmann constant, and μ_g is the chemical potential controlled by the doping. Since the distribution of the doping density across the width of graphene nanoribbon is quite nonuniform,[43,44] we use the one-dimensional carrier density n_0 along a graphene nanoribbon. Follow Refs. 31 and 47 the chemical potential can be calculated as $\mu_g = \pi\hbar v_F n_0/2$,

where n_0 is the one-dimensional carrier density, and $v_F = \sqrt{3}a_0 t/(2\hbar) \approx 10^8$ cm/s is the Fermi velocity of electrons in graphene, where $a_0 = 2.46$ Å is a lattice constant and the value of the overlap integral between the nearest carbon atoms is $t \approx 2.71$ eV.[48] The one-dimensional carrier density is $n_0 = 2k_F/\pi$,[31,47] where k_F is the Fermi wave vector. In Ref. 31 $n_0 = 2.8 \times 10^7$–5.6×10^7 m^{-1} were used that correspond to the values of Fermi wave vector in the range of $k_F a_0 = 0.0108$–0.0216. In our calculations we use n_0 the same order of magnitude as in Ref. 31.

We emphasize that the proposed in Eqs. (A1) and (A2) form for the dielectric function taking into account the damping rate γ gives the exact correspondence with Eq. (8) in Ref. 49, where the dielectric function with the damping rate was introduced.

The Coulomb matrix element $V_{0,0}(q_x)$ is given by[31]

$$V_{0,0}(q_x) = \int_0^1 du \int_0^1 du' V(q_x W|u-u'|), \qquad \text{(A4)}$$

where W is the width of graphene nanoribbon in the y direction. The one-dimensional Fourier transform of the Coulomb interaction has the form[50]

$$V(q_x|y-y'|) = \frac{2ke^2}{\varepsilon_g} K_0(q_x|y-y'|), \qquad \text{(A5)}$$

where e is the charge of an electron, $\varepsilon_g = 2.5$ is the static dielectric constant of graphene, and $K_0(y)$ is the zeroth-order modified Bessel function of the second kind, which diverges as $-\ln y$ when y goes to zero.

Substituting Eq. (A5) for $V(q_x W|u-u'|)$ into Eq. (A4) we obtain

$$V_{0,0}(q_x) = \frac{2ke^2}{\varepsilon_g} \int_0^1 du \int_0^1 du' K_0(q_x W|u-u'|). \qquad \text{(A6)}$$

We are interested in obtaining the dynamical dielectric function at the frequencies $\omega \gg v_F k$. After the substitution of $\Pi_{0,0}(q_x,\omega,\beta,\mu_g)$ from Eq. (A2) and $V_{0,0}(q_x)$ from Eq. (A6) into Eq. (A1), and taking into account Eq. (A3), one can obtain the dielectric function for the graphene nanoribbon.

APPENDIX B: THE ELECTRIC FIELD OF A PLASMON IN A GRAPHENE NANORIBBON

$\vec{E}(x,y,z)$ can be found from the equation

$$\mathrm{div}\vec{D}(x,y,z) = \frac{\partial D_x(x,y,z)}{\partial x} + \frac{\partial D_y(x,y,z)}{\partial y} + \frac{\partial D_z(x,y,z)}{\partial z} = 0. \qquad \text{(B1)}$$

If there are two materials contacting each other along the plane there are the boundary conditions at the plane of the contact: $D_{n1} = D_{n2}$ and $E_{t1} = E_{t2}$, where D_{n1} and D_{n2} are the normal to the contact plane components of $\vec{D}$, and E_{t1} and E_{t2} are tangent to the contact plane components of $\vec{E}$.

Using the notation $u = x - x'$, $v = y - y'$, we have

$$\vec{D}(x,y,z) = \begin{cases} \int_{-\infty}^{+\infty} du \int_{-W/2}^{+W/2} dv \varepsilon(u,v) \vec{E}(x-u,y-v,z) & \text{at } z = 0 \text{ and } -W/2 < y < W/2 \\ \varepsilon_d \vec{E}(x,y,z) & \text{at } z < 0 \text{ or } z > 0 \text{ or } y < -W/2 \text{ or } y > W/2 \end{cases}. \qquad \text{(B2)}$$

At $z = 0$ and $-W/2 < y < W/2$ we have from Eqs. (B1) and (B2)

$$\int_{-\infty}^{+\infty} du \int_{-W/2}^{+W/2} dv\, \varepsilon(u,v) \left(\frac{\partial E_x(x-u,y-v,z)}{\partial x} + \frac{\partial E_y(x-u,y-v,z)}{\partial y} + \frac{\partial E_z(x-u,y-v,z)}{\partial z} \right) = 0, \qquad \text{(B3)}$$

which can be presented as

$$\int_{-\infty}^{+\infty} du \int_{-W/2}^{+W/2} dv\, \varepsilon(u,v) \mathrm{div}\vec{E}(x-u,y-v,z) = 0. \qquad \text{(B4)}$$

If we do the Fourier transformation of Eq. (B4) and use the property of the Fourier image of the convolution, assuming that inside the graphene nanoribbon the medium is homogeneous, we obtain

$$\mathrm{div}\vec{E}(x,y,z) = 0. \qquad \text{(B5)}$$

Let us mention that for $z < 0$ and $z > 0$ or $y < -W/2$ and $y > W/2$ it is obvious that Eq. (B5) follows from Eqs. (B1) and (B2).

If we define the potential $\vec{E}(x,y,z) = -\nabla\varphi(x,y,z)$, we obtain from Eq. (B5) for $z < 0$ and $z > 0$

$$\Delta\varphi(x,y,z) = 0. \qquad \text{(B6)}$$

The solution of Eq. (B6) for $z \neq 0$ will be written as

$$\varphi(x,y,z) = \psi\left(k_x x + k_y y \pm i\sqrt{k_x^2 + k_y^2}|z|\right) = \psi(v), \qquad \text{(B7)}$$

where $v = k_x x + k_y y \pm i\sqrt{k_x^2 + k_y^2}|z|$. Then we have for $\vec{E}(x,y,z)$ where $\psi' = d\psi(v)/dv$,

$$\vec{E}(x,y,z) = -\psi'\left(k_x x + k_y y \pm i\sqrt{k_x^2 + k_y^2}|z|\right)\vec{b}_0, \qquad \text{(B8)}$$

where $\vec{b}_0 = [k_x, k_y, \pm i\,\mathrm{sign}(z)\sqrt{k_x^2 + k_y^2}]$. From the boundary conditions we have $k_x = iq_x$, $k_y = \pm iq_y$, where for the armchair nanoribbon we have from Ref. 30 $q_{ym} = 2\pi/(3a_0)\,[(2M+1+m)/(2M+1)]$ at the width $W = (3M+1)a_0$, where a_0 is the graphene lattice constant defined above, and m is the integer. We use $m = 1$.

Defining $\alpha = \sqrt{q_x^2 + q_y^2}$ and using $\psi(w) = E_0 e^w/2$, we obtain for $\vec{E}(x,y,z)$ from Eq. (B8):

$$\vec{E}(x,y,z) = -\frac{E_0}{2} e^{iq_x x - \alpha|z|}\left(e^{iq_y y}\vec{b}_1 + e^{-iq_y y}\vec{b}_2\right), \qquad \text{(B9)}$$

where $\vec{b}_1 = [iq_x, iq_y, -\alpha\,\mathrm{sign}(z)]$ and $\vec{b}_2 = [iq_x, -iq_y, -\alpha\,\mathrm{sign}(z)]$.

[1]D. J. Bergman and M. I. Stockman, Phys. Rev. Lett. **90**, 027402 (2003).
[2]M. I. Stockman, J. Opt. **12**, 024004 (2010).
[3]I. E. Protsenko, Phys. Usp. **55**, 1040 (2012).
[4]V. M. Agranovich and V. L. Ginzburg, *Crystal Optics With Spartial Dispersion, and Excitons* (Springer, Berlin, 1984).
[5]Yu. E. Lozovik and A. V. Klyuchnik, *The Dielectric Function and Collective Oscillations Inhomogeneous Systems*, in *The Dielectric Function of Condensed Systems*, edited by L. V. Keldysh, D. A. Kirzhnitz, and A. A. Maradudin (Elsevier, Amsterdam, 1987), p. 299.
[6]A. V. Zayats, I. I. Smolyaninov, and A. A. Maradudin, Phys. Rep. **408**, 131 (2005).
[7]D. K. Gramotnev and S. I. Bozhevolnyi, Nat. Photon. **4**, 83 (2010).
[8]M. I. Stockman, Nat. Photon. **2**, 327 (2008).
[9]A. A. Lisyansky, I. A. Nechepurenko, A. V. Dorofeenko, A. P. Vinogradov, and A. A. Pukhov, Phys. Rev. B **84**, 153409 (2011).
[10]E. S. Andrianov, A. A. Pukhov, A. V. Dorofeenko, A. P. Vinogradov, and A. A. Lisyansky, Opt. Lett. **36**, 4302 (2011).
[11]E. S. Andrianov, A. A. Pukhov, A. V. Dorofeenko, A. P. Vinogradov, and A. A. Lisyansky, Opt. Express **19**, 24849 (2011).
[12]E. S. Andrianov, A. A. Pukhov, A. V. Dorofeenko, A. P. Vinogradov, and A. A. Lisyansky, Phys. Rev. B **85**, 035405 (2012).
[13]E. S. Andrianov, A. A. Pukhov, A. V. Dorofeenko, A. P. Vinogradov, and A. A. Lisyansky, Phys. Rev. B **85**, 165419 (2012).
[14]D. G. Baranov, E. S. Andrianov, A. P. Vinogradov, and A. A. Lisyansky, Opt. Express **21**, 10779 (2013).
[15]A. Noginov, G. Zhu, V. P. Drachev, and V. M. Shalaev, in *Nanophotonics With Surface Plasmons*, edited by V. M. Shalaev and S. Kawata (Elsevier, Amsterdam, 2007).
[16]M. A. Noginov, G. Zhu, A. M. Belgrave, R. Bakker, V. M. Shalaev, E. E. Narimanov, S. Stout, E. Herz, T. Suteewong, and U. Wiesner, Nature (London) **460**, 1110 (2009).
[17]N. I. Zheludev, S. L. Prosvirnin, N. Papasimakis, and V. A. Fedotov, Nat. Photon. **2**, 351 (2008).
[18]E. Plum, V. A. Fedotov, P. Kuo, D. P. Tsai, and N. I. Zheludev, Opt. Express **17**, 8548 (2009).
[19]R. A. Flynn, C. S. Kim, I. Vurgaftman, M. Kim, J. R. Meyer, A. J. Mäkinen, K. Bussmann, L. Cheng, F.-S. Choa, and J. P. Long, Opt. Express **19**, 8954 (2011).
[20]L. A. Falkovsky and A. A. Varlamov, Eur. Phys. J. B **56**, 281 (2007).
[21]L. A. Falkovsky and S. S. Pershoguba, Phys. Rev. B **76**, 153410 (2007).
[22]L. A. Falkovsky, J. Phys.: Conf. Ser. **129**, 012004 (2008).
[23]F. H. L. Koppens, D. E. Chang, and F. J. G. de Abajo, Nano Lett. **11**, 3370 (2011).
[24]A. H. Castro Neto, F. Guinea, N. M. R. Peres, K. S. Novoselov, and A. K. Geim, Rev. Mod. Phys. **81**, 109 (2009).
[25]S. Das Sarma, S. Adam, E. H. Hwang, and E. Rossi, Rev. Mod. Phys. **83**, 407 (2011).
[26]E. H. Hwang and S. Das Sarma, Phys. Rev. B **75**, 205418 (2007).
[27]Yu. E. Lozovik, Phys. Usp., **55**, 1035 (2012).
[28]S. A. Mikhailov, Phys. Rev. B **87**, 115405 (2013).
[29]V. G. Kravets, F. Schedin, R. Jalil, L. Britnell, R. V. Gorbachev, D. Ansell, B. Thackray, K. S. Novoselov, A. K. Geim, A. V. Kabashin, and A. N. Grigorenko, Nat. Mater. **12**, 304 (2013).
[30]L. Brey and H. A. Fertig, Phys. Rev. B **73**, 235411 (2006).
[31]L. Brey and H. A. Fertig, Phys. Rev. B **75**, 125434 (2007).
[32]V. V. Popov, T. Yu. Bagaeva, T. Otsuji, and V. Ryzhii, Phys. Rev. B **81**, 073404 (2010).
[33]O. L. Berman, V. S. Boyko, R. Ya. Kezerashvili, A. A. Kolesnikov, Yu. E. Lozovik, Phys. Lett. A **374**, 4784 (2010).
[34]O. L. Berman and R. Ya. Kezerashvili, J. Phys.: Condens. Matter **24**, 015305 (2012).
[35]O. L. Berman, R. Ya. Kezerashvili, and Yu. E. Lozovik, Bulletin of APS **58**(1), W5.00004, March 18–22, 2013.
[36]R. H. Good, *Classical Electromagnetism* (Saunders College, Orlando, FL, 1999).
[37]L. D. Landau and E. M. Lifshitz, *Electrodynamics of Continuous Media* (Pergamon, Oxford, 1984).
[38]P. Neugebauer, M. Orlita, C. Faugeras, A. L. Barra, and M. Potemski, Phys. Rev. Lett. **103**, 136403 (2009).
[39]M. Orlita and M. Potemski, Semicond. Sci. Technol. **25**, 063001 (2010).
[40]A. A. Dubinov, V. Ya. Aleshkin, V. Mitin, T. Otsuji, and V. Ryzhii, J. Phys.: Condens. Matter **23**, 145302 (2011).
[41]N. K. Emani, T.-F. Chung, X. Ni, A. V. Kildishev, Y. P. Chen, and A. Boltasseva, Nano Lett. **12**, 5202 (2012).
[42]M. I. Stockman, SPIE Proc. **4992**, 60 (2003).
[43]P. G. Silvestrov and K. B. Efetov, Phys. Rev. B **77**, 155436 (2008).
[44]S. Thongrattanasiri, I. Silveiro, and F. Javier Garcí a de Abajob, Appl. Phys. Lett. **100**, 201105 (2012).
[45]J. M. Auxier, A. Schülzgen, M. M. Morrell, B. R. West, S. Honkanen, S. Sen, N. F. Borrelli, and N. Peyghambarian, SPIE Proc. **5709**, 249 (2005).
[46]I. A. Larkin, M. I. Stockman, M. Achermann, and V. I. Klimov, Phys. Rev. B **69**, 121403(R) (2004).
[47]D. R. Andersen and H. Raza, Phys. Rev. B **85**, 075425 (2012).
[48]V. Lukose, R. Shankar, and G. Baskaran, Phys. Rev. Lett. **98**, 116802 (2007).
[49]N. D. Mermin, Phys. Rev. B **1**, 2362 (1970).
[50]Q. P. Li and S. Das Sarma, Phys. Rev. B **43**, 11768 (1991).